

Moisture content and strain relation in wood by Bragg grating sensor and unilateral NMR

Luca Senni · Michele Caponero · Cinzia Casieri ·
Ferdinando Felli · Francesco De Luca

Received: 21 November 2008 / Published online: 15 July 2009
© Springer-Verlag 2009

Abstract The paper describes a low-invasive experimental apparatus designed for the accurate determination of mechanical deformation and moisture content (MC) relationship on macroscopic wood samples. The device is particularly indicated for monitoring wooden handwork whose mechanical deformation is especially critical in relation to its role such as, for example, works of art or architectural works. The MC of wood is measured with a portable single-sided NMR probe and mechanical deformation by a fiber Bragg grating optical sensor. The data obtained are of high accuracy, despite the dimensions of the sample. The methodology provides an effective tool for investigating the dynamic relation between environmental relative humidity, MC, and shrinking–swelling of wood. Adsorption results collected for longitudinal deformation in silver fir (*Abies alba* Mill.) are presented to show the sensitivity of the optical sensor. Interesting findings include the detection of two different mechanisms of elongation and the time evolution of water mobility versus hydration and strain.

L. Senni · F. De Luca (✉)
Dipartimento di Fisica, Università “La Sapienza”, P.le Aldo Moro 2, 00185 Rome, Italy
e-mail: francesco.deluca@roma1.infn.it

M. Caponero
ENEA CR Frascati, Via Enrico Fermi 45, 00044 Frascati, RM, Italy

C. Casieri
Dipartimento di Fisica, Università di L’Aquila, V. Vetoio 10, 67010 Coppito, L’Aquila, Italy

F. Felli
Dipartimento ICMMPM, Università “La Sapienza”, Via Eudossiana 18, 00184 Rome, Italy

C. Casieri · F. De Luca
Centro SOFT-INFN-CNR, Università “La Sapienza”, P.le Aldo Moro 2, 00185 Rome, Italy

Introduction

It is well known that the stress–strain behavior of wood depends strictly on its hydration state. Wood behaves like fragile material in low-hydration state, whereas at higher hydration it adopts plastic properties very similar to those of a metal; moreover, it also behaves like an orthotropic material, that is, the mechanical behavior in the longitudinal, radial and tangential axes are almost independent (Keckes et al. 2003; Ishimara et al. 2001). These uncommon mechanical properties completely depend on the hierarchic structure of wood, which ranges from the centimeter of the macroscopic annual ring structure to the Å of cellobiose molecular scale. Water plays the role of a kind of hydrogen-bonding intermediary between molecules and it is determinant in the formation of the interconnections between different structures because it may mediate the formation of hydrogen bonds between the hydroxyl groups of macromolecules. Water also forms clusters that predominantly reside between fibrils (Skaar 1988; Wood Handbook 1987; Reeb 1995).

Variations of temperature and environmental relative humidity may modify the moisture content (MC) of wood producing anisotropic shrinking–swelling on account of its orthotropic character. This behavior is more or less present in any wood species, and it may notably influence the practical utilization of wood. Some important examples are the cultural heritage handwork and architectural works, which both are particularly sensitive to volumetric deformation: works of art may loose their esthetic quality, while architectural elements may change proper geometrical relationships, thus, modifying their functional shapes (Senni et al. 2008). Therefore, the knowledge of the orthotropic characteristics is of central concern to foresee the behavior of wooden items operating under different conditions (Jakiela et al. 2008).

In this paper, a novel experimental set up for volumetric deformation measurements of wood handwork in relation to their hydration state is presented. It is based on a mobile NMR sensor, which may give precise response on MC of wood, and an optical sensor, based on the Bragg diffraction, which may measure linear dimension variation up to nanometer scale.

Fiber Bragg gratings (FBGs) are realized by producing a periodic spatial variation on refractive index in a segment of an optical fiber (Kashyap 1999). The grating acts as a selective mirror that only reflects a certain range of the light wavelength traveling through the fiber. It is the wavelength λ_B that makes the Bragg constructive interference to occur. The Bragg condition is reached for $\lambda_B = 2n_{\text{eff}}\Lambda$, where n_{eff} is the effective refractive index of the fiber and Λ the axial grating pitch of refractive index. Therefore, any variation affecting Λ , like for example, strain on the fiber, shifts the Bragg wavelength. The shift can easily be monitored and related to the strain of sample over which the Bragg sensor is rigidly mounted. The modality of fixing the sensor on the sample, which typically takes place by gluing, constitutes the only invasive aspect of the whole apparatus. The Bragg sensors may provide microstrain ($\mu\epsilon$) resolution, thus being potentially sensitive to nanometer axial elongation on millimeter scale, and it is immune to electrostatic and radiofrequency interferences (Rao 1999).

A portable and non-invasive NMR probe may furnish all low-resolution NMR data on wood, independent of the sample dimensions (Eidmann et al. 1996; Casieri et al. 2005; Viola et al. 2004; Camaiti et al. 2007; Cignini et al. 2006; Fechete et al. 2003; Bortolotti et al. 2006). The single-sided NMR apparatus consists of two permanent magnets in open geometry producing low-intensity- and low-homogeneity magnetic fields (Anferova et al. 2002). The probe is characterized by a spatial selectivity, the sensitive volume, defined by the volume where NMR resonant conditions are fulfilled. Such a peculiarity allows for measuring the NMR parameters in a fixed volume of the sample. The moisture in wood is obtained by measuring the moisture volume fraction, which corresponds to the sensitive volume fraction filled by water (Casieri et al. 2004). With this parameter and the specific gravimetric factor of dried wood, the MC defined as ratio of water mass to that of anhydrous wood might be obtained. Moreover, by means of the inverse Laplace transform of relaxation curves, it is possible to collect information on the evolution of water mobility during the hydration process and its relation to mechanical strain along a selected direction, or along different directions simultaneously.

In the paper, the main characteristics of the apparatus are shown. Water adsorption measurements together with longitudinal strain measurements in silver fir (*Abies alba* Mill.) are reported to show the sensitivity of the experimental set up and its versatility. The kinetics of water adsorption was studied by following sample hydration from dry condition to equilibrium at 85% RH and 23°C: variation of MC and strain were correlated utilizing the spin–spin relaxation time and the nuclear magnetization, with the latter being directly related to MC. At short hydration times, the strain deviates from the one expected by MC behavior allowing for supposing two different strain mechanisms with different water mobility.

Materials and methods

The NMR sensor is the mq-ProFiler (Bruker Biospin, Italy) with a ^1H resonant frequency of 15.8 MHz. The spatial selectivity of the sensor (sensitive volume) is a layer of about 3 mm from the permanent magnets plane with a surface of about $8 \times 20 \text{ mm}^2$. The magnetic field has a parabolic-like distribution with local linear gradient intensities of up to 10 T/m.

The moisture volume fraction Θ is defined by (Casieri et al. 2004)

$$\Theta = \frac{V_W}{V_S} = \frac{V_W \rho_W}{V_S \rho_W} = \frac{M_0}{M_{0S}} \quad (1)$$

where V_W is the volume occupied by water, V_S the sensitive volume of the sensor, ρ_W the magnetization density of water, M_0 the equilibrium magnetization of water taking up the volume V_W : it is related to the number of protons in V_W . M_{0S} is the equilibrium magnetization of water filling up the volume V_S . V_S and M_{0S} are constants of the sensor; hence, the fraction of volume occupied by water is measured directly by measuring M_0 . By multiplying Θ for the ratio between the density of water and that of dried wood that is by dividing Θ by the specific gravity

factor of dried wood, MC is obtained. Because $MC(t)$ is of interest, $MC(t)$ will directly be expressed by $M_0(t)$.

Spin–spin relaxation (T_2) distribution was measured with CPMG pulse sequence (Meiboom and Gill 1958), with inter pulse delay corresponding to echo time $\tau_E = 44 \mu\text{s}$.

Recent silver fir (*Abies alba* Mill.) wood specimens of $18 \times 18 \times 210 \text{ mm}^3$ were prepared. The samples were dried in a silica gel desiccator for 1 month at a temperature of $23 \pm 1^\circ\text{C}$. An FBG sensor was applied parallel to the wood grain direction (longitudinal axis). The FBG was glued rigidly on the wood sample. The dried sample with the FBG sensor was put in an 85% relative humidity chamber at $23 \pm 1^\circ\text{C}$; NMR measurements were performed inside the chamber during the hydration process to avoid alteration of measurement conditions. Measurements were conducted for about 400 h. Weight of the sample was monitored to confirm reaching of equilibrium condition. PC controlled sensors continuously monitored relative humidity and temperature.

The FBG diffraction grating took a segment of 5 mm in length, with a fiber diameter of 0.25 mm. The FBG was produced in telecom grade monomodal optical fiber, with grating pitch intended to operate within 1,520–1,560 nm. The Bragg diffraction was made to occur as a narrow-band back-reflection with 0.1 nm FWHM and 90% diffraction efficiency.

The shift $\Delta\lambda_B$ of Bragg wavelength is related to strain ε by

$$\Delta\lambda_B = 2n_{\text{eff}}\Lambda(1 + n_{\text{eff}}^2P)\varepsilon \quad (2)$$

where P represents the term due to the Pockels and Posson factors. Typically, it may be written as

$$\varepsilon = \frac{\Delta L}{L_0} \cong \frac{\Delta\lambda_B}{0.78\lambda_B} \quad (3)$$

where ΔL is the spatial elongation parallel to the sensor axis with respect to the starting value L_0 . Considering the use of telecom grade-silica optical fibers FBG operating in the standard III telecom window (1,520/1,560 nm), Eq. 3 gives $\Delta\lambda_B = 1 \text{ pm}$ for $\Delta\varepsilon \approx 0.8 \mu\varepsilon$. Because the resolution of $\Delta\lambda_B = 1 \text{ pm}$ can be obtained by commercially available FBG interrogation system, the resolution of $\Delta L \approx 1 \text{ nm}$ for $L_0 \approx 1 \text{ mm}$ can be confidently assumed.

In Fig. 1, the scheme of the experimental set up is presented.

Results and discussion

The experimental results concerning longitudinal strain, relative variations of magnetization $[M_0(t) - M_0(0)]/M_0(0)$ and spin–spin relaxation time $[T_2(t) - T_2(0)]/T_2(0)$ of the silver fir specimen during moisture uptake are shown in Fig. 2. The time axis indicates the residence time of the sample in the hydration chamber at 85% relative humidity and $T = 23 \pm 1^\circ\text{C}$; zero time corresponds to the time when the dried sample was placed in the chamber. Although measurements were realized under non-equilibrium condition, it can be assumed that from an NMR parameter

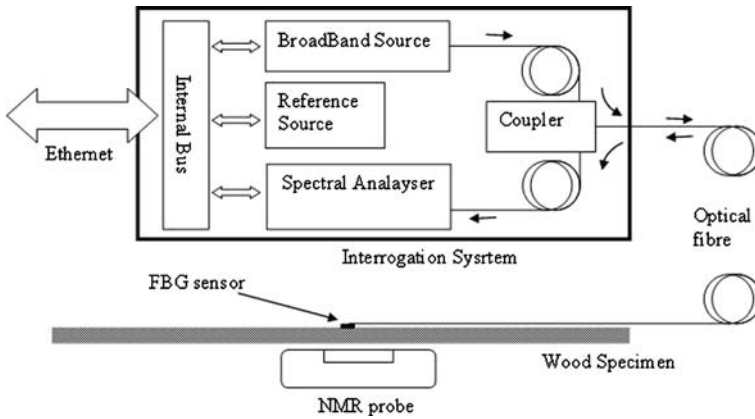


Fig. 1 Schematic view of the FBG sensor apparatus and the NMR sensor

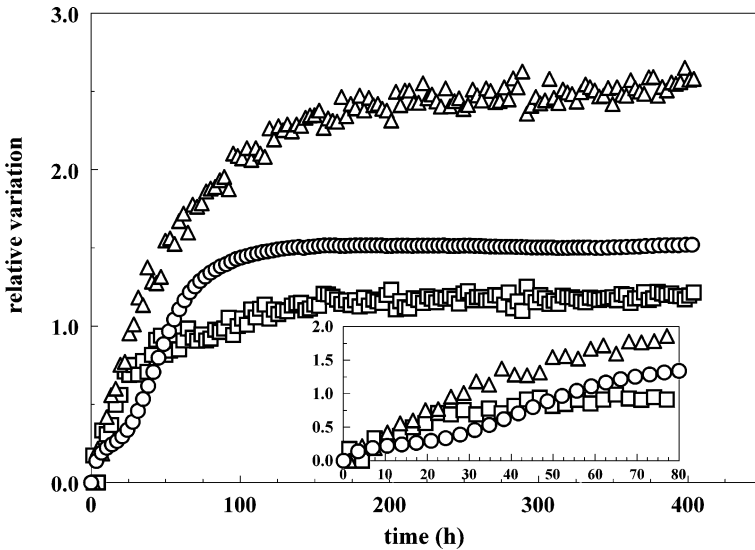


Fig. 2 Experimental relation between the relative variation $[M_0(t) - M_0(0)]/M_0(0)$ of equilibrium magnetization (*triangles*), the relative variation $[T_2(t) - T_2(0)]/T_2(0)$ of spin–spin relaxation time (*squares*) and the longitudinal strain ϵ (*circles*) of the silver fir specimen as a function of the hydration time in hours. The *inset* magnifies the short hydration time data

point of view the sample was basically in equilibrium, since the characteristic time related to magnetization equilibrium dynamics (T_1 or spin–lattice relaxation time) of water was of the order of milliseconds, while the time parameter characterizing the hydration mechanism was of the order of hours.

In this view, $M_0(t)$ indicates the equilibrium magnetization of adsorbed water measured at the hydration time t ; this is also valid for $T_2(t)$, being always $T_1 \geq T_2$. $M_0(t)$ is extrapolated from the spin-echo CPMG data and it is a direct measure of

MC (Eq. 1). In measurements on wood, protons from macromolecules may also contribute to the magnetization signal (Almeida et al. 2006). This contribution is generally characterized by much shorter T_2 than T_2 of water and it may be filtered off from the whole signal. However, because protons of macromolecules do not change during hydration, their contribution to $M_0(t)$ and $T_2(t)$ can be ignored.

The sample adsorbs water (Fig. 2) with a characteristic time $T_0 \approx 40$ h obtained by fitting the experimental data with the relation

$$\frac{M_0(t) - M_0(0)}{M_0(0)} = k \left(1 - \exp\left(-\frac{t}{T_0}\right) \right) \quad (4)$$

where k is a dimensionless constant that depends on the asymptotic value of data. An analogous relation works for $T_2(t)$, with a characteristic time $T_0 \approx 50$ h quite close to that of $M_0(t)$. The closeness between the characteristic times of $M_0(t)$ and $T_2(t)$ is not surprising, because with increase in the amount of water, it also increases the water mobility and therefore $T_2(t)$.

Apart from the so-called free water found in the lumen of wood, which in practice is only found in living trees, it is possible to make a schematic division of water adsorbed in the cell wall of wood. Water may directly be entangled with macromolecules, owing to hydrogen bonds formation with the hydroxyl groups of cellulose, hemicelluloses, and lignin; this bound water (BW) is not as mobile as the free one and it has a rather short T_2 . More mobile water is associated with molecules forming water clusters within cellulose fibrils and amorphous regions of cellulose chains. The number and dimension of clusters, typically composed of few molecules, augment to values that depend on wood species and environmental thermo-hygrometric conditions. This quasi-bound water (QBW) is more mobile than BW, although still less mobile than free water, and it also has longer T_2 than BW.

The strain shows a behavior fully compatible with $M_0(t)$ and $T_2(t)$, but at short hydration time (Fig. 2). In this range, the strain seems to have two different characteristics: below about 10 h, its amplitude remains quite low, while above 20 h the increase is markedly higher, and between 10 and 20 h it remains quite constant. The elongation in function of M_0 and T_2 , which are indicative of MC and water mobility, respectively, confirms this behavior (Figs. 3, 4). Apart from the clear non-linear relation between elongation and MC, in the data of Figs. 3, 4, two different characteristics may be identified as well: one giving low elongation, $\Delta L \approx 1 \mu\text{m}$ with $\Delta M_0 \approx 5$ a.u. or $\Delta T_2 \approx 0.2$ ms, and another giving $\Delta L \approx 6 \mu\text{m}$ for about the same variation of M_0 and T_2 . It comes natural to assign the low-elongation regime to BW and the high one to the QBW effect because the adsorbing force related to hydrogen bonds drives water to form primarily hydrogen bonds with the OH groups of macromolecules, and subsequently, with the reduction in the hydrogen binding sites, the formation of water clusters. Actually, the two processes are superimposed, but at a short time hydrogen bonding has higher probability to be set. In this view, the elongation during hydration may be described by the function:

$$\Delta L = \Delta L_{01} \left(1 - \exp\left(-\frac{t}{T_{01}}\right) \right) + \Delta L_{02} P(t - t_D) \left(1 - \exp\left(-\frac{t}{T_{02}}\right) \right) \quad (5)$$

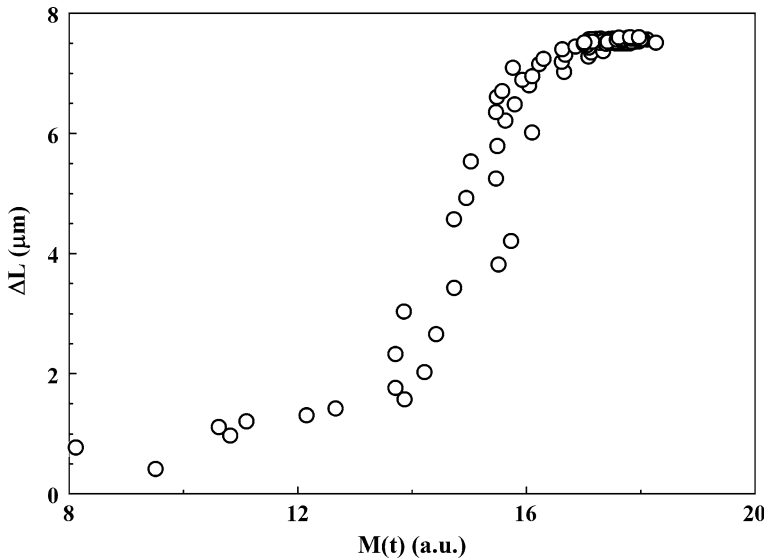


Fig. 3 The longitudinal sample elongation, referred to the FBG sensor dimension (5 mm), as a function of nuclear magnetization

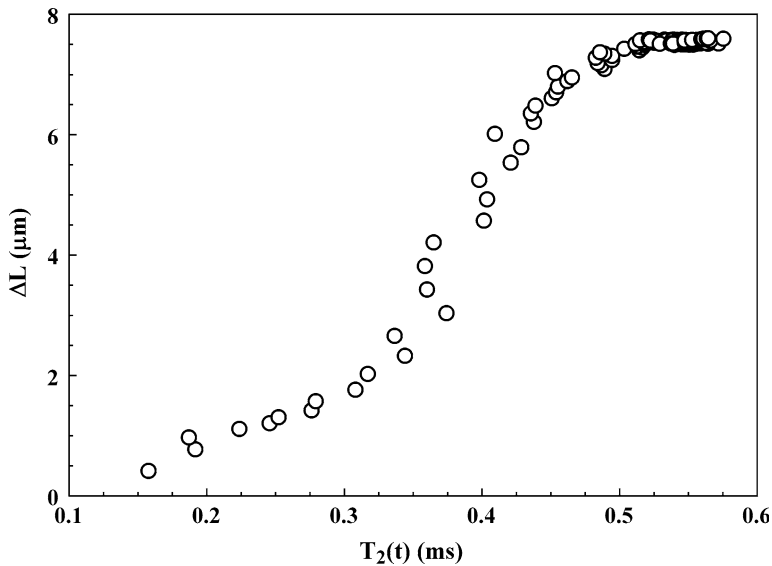


Fig. 4 The longitudinal sample elongation, referred to the FBG sensor dimension (5 mm), as a function of T_2

where ΔL_{01} and ΔL_{02} are, respectively, the equilibrium ($t \rightarrow \infty$) elongation associated with BW and QBW, T_{01} and T_{02} are the time constants characterizing the two hydration mechanisms and $P(t - t_D)$ is the time-dependent probability of the

QBW mechanism setting: t_D is the time when the probability of QBW mechanism reaches $1/2(P(t - t_D)) \propto \tanh(C(t - t_D))$, where C is related to the probability growing rate. The results of fit are reported in Fig. 5. Eq. 5 is very effective and numerical results give $\Delta L_{01} \cong 0.9 \mu\text{m}$ (or approx. $180 \mu\text{e}$), $\Delta L_{02} \cong 6.6 \mu\text{m}$ (or approx. $1,320 \mu\text{e}$), $T_{01} \cong 3 \text{ h}$, $T_{02} \cong 30 \text{ h}$ and $t_D = 40 \text{ h}$. This means that the elongation is practically entirely associated with the QBW mechanism and approx. 3 h is the time characterizing hydrogen bonding, while 30 h is the one characterizing clusters formation. Moreover, t_D indicates that the QBW mechanism is particularly effective for elongation if, from a probability point of view, it becomes significant only after about 40 h. On the other hand, the latter coincides with the one characterizing $M_0(t)$: this seems to indicate that the hydration of wood is more characterized by cluster formation than by hydrogen bonding.

The physical properties of adsorbed water are better understood if the behavior of $T_2(t)$ is observed in detail. $M_0(t)$ does not show any particular behavior that might indicate the change in the elongation regime at short hydration time (Fig. 2): this is expected since the addition of water molecules change the magnetization independently if water plays the role of BW or QBW. Apparently, it seems the same for T_2 (Fig. 2), but T_2 , differently by $M_0(t)$, should instead distinguish between BW and QBW since T_2 is related to water mobility and hence to water interaction with wood structures.

The T_2 data utilized in Figs. 2 and 4 are geometrical, that is, the average T_2 obtained by weighting the relaxation time with proper spin population. The distribution of T_2 relatively to the spin population is given by the inverse Laplace transform of relaxation curve (Borgia et al. 1998), which supplies the spin

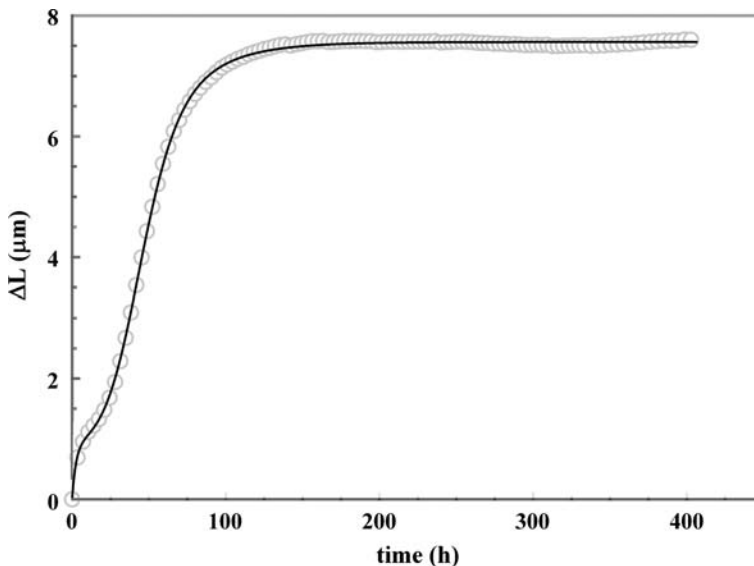


Fig. 5 The experimental data of sample elongation, as a function of the hydration time, fitted by Eq. 5 (full line)

population per T_2 interval, or signal density. The geometrical T_2 is little sensitive to small asymmetrical variation in the T_2 range and, therefore, the T_2 differences related to the different hydration mechanism are attenuated. If, however, one looks directly at the T_2 distribution, the relaxation evolution may be put in better evidence and in more detail. The T_2 distribution obtained by the inverse Laplace transform of experimental relaxation curves, as a function of the hydration time, is shown in

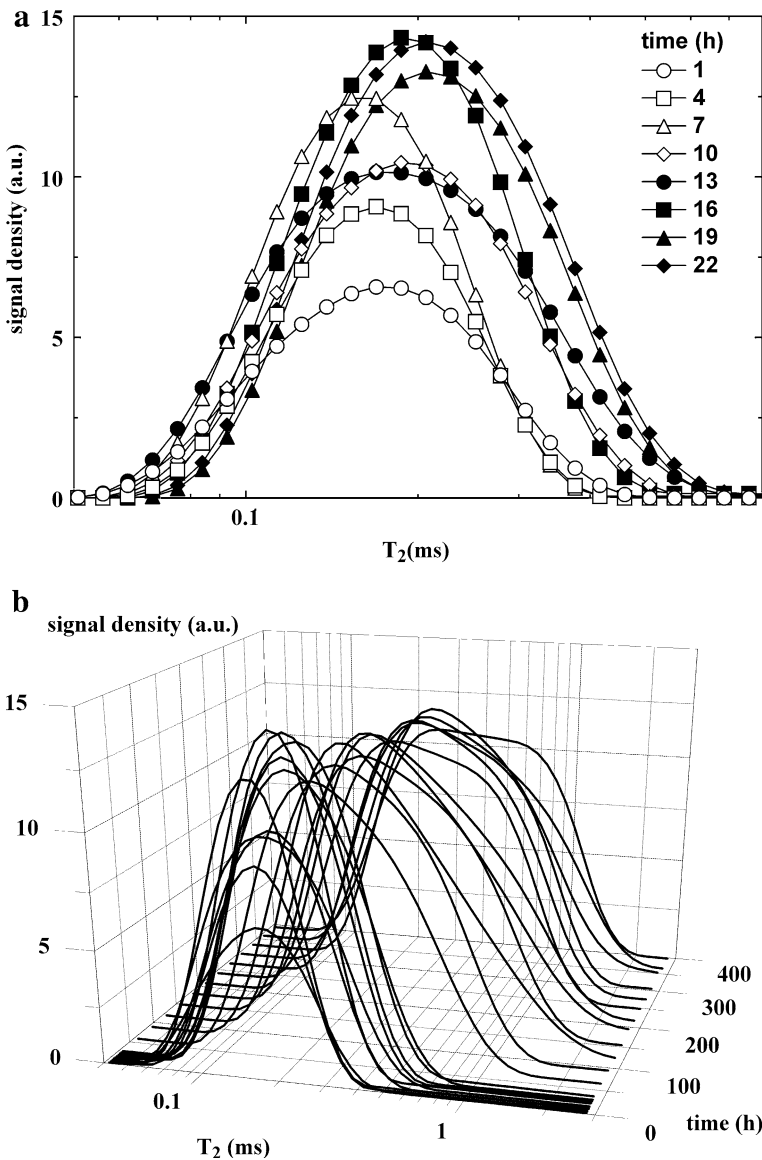


Fig. 6 **a** Short hydration time T_2 distribution. **b** Full hydration time T_2 distribution

Fig. 6a for short hydration time. It is easy to see that at around 10 h there is a “jump” of the T_2 range, which enlarges to the longer T_2 side. Before this time, the curves remain constant in width, while the changes in amplitude reflect only the quantity of adsorbed water. This indicates that at around 10 h a new hydration mechanism appears (see also Fig. 2), which characterized by higher water mobility that seems the early detection of the QBW mechanism. This is confirmed by Fig. 6b, where the entire range of hydration time is reported. Figure 6b shows that above approx. 30 h, T_2 enlarges more towards the higher mobility side, confirming the time range where the QBW mechanism becomes significant.

Conclusion

A new method to evaluate contemporaneously MC and the directional strain of wood with high precision, and with low-invasive impact, is presented. The method makes it possible to study the relations between environmental relative humidity, water sorption and dimensional changes of wood handwork. It allows for measuring under non-equilibrium and in situ conditions without particular logistic obstacles. The experimental capabilities of the method include the detection of the hydration mechanisms and the modality of strain, also along the three main directions of wood. Because a large number of FBG sensors may be utilized simultaneously, strain measurements may involve different directions of interest, besides the main ones. The combination of NMR single-sided and FBG sensor may, on the one hand, allow studying basic adsorption mechanisms on macroscopic samples and gaining insight into the physics of strain during hydration; and, on the other hand, they may also be utilized for monitoring specific aspects of wood objects in specific environmental situations. The invasivity of the device is really low, and it concerns only the modality of fixing the FBG sensor on the handwork. This aspect may, however, be studied for specific applications, taking into account that handwork may differently support the invasive effect of the device: cultural heritage objects have strict drawbacks while architectural works may support a higher degree of invasivity.

The results obtained in this paper directly connect the hydration to mechanical deformations, with details concerning the microscopic role of water. Notwithstanding its simplicity, the apparatus may allow a systematic study of wood specimens addressed to getting full correlation of $M_0(t)$ or $T_2(t)$ with strain and therefore preventing deformation just by MC testing and, possibly, by T_2 distribution. Such a monitoring may allow foreseeing mechanical behavior of wood in a complete non-invasive way.

In this paper, only measurements in one wood direction are presented, but it is easy to measure strain contemporary along three or more directions being different FBG which can be used simultaneously in a very large number. Therefore, all tensorial wood characteristics relative to strain and hydration may be measured easily. Moreover, the stress–strain relation might also be studied effectively, also for what concerns the microscopic rearrangement of water under stress condition.

Acknowledgments We thank Paola Fantazzini who supplied us with UPEN algorithm to get inverse Laplace transform of relaxation data. Thanks are due to Sergio Ciuchi for suggestions regarding Eq. 5. All of us are indebted to Bruker BioSpin S.r.L., Milan, Italy, for the assistance and updating of the NMR sensor.

References

- Almeida G, Gagne S, Hernandez RE (2006) A NMR study of water distribution in hardwoods at several equilibrium moisture contents. *Wood Sci Technol* 41:293–307
- Anferova S, Anferov V, Adams M, Blumler P, Routley N, Hailu K, Kupferschlager K, Mallett MJD, Schroeder G, Sharma S, Blumich B (2002) Construction of a NMR-MOUSE with short dead time. *Concept Magn Reson* 15:15–25
- Borgia GC, Brown RJS, Fantazzini P (1998) Uniform-penalty inversion of multiexponential decay data. *J Magn Reson* 132:65–77
- Bortolotti V, Camaiti M, Casieri C, De Luca F, Fantazzini P, Terenzi C (2006) Water absorption kinetics in different wettability conditions studied at pore and sample scales in porous media by NMR with portable single-sided and laboratory imaging devices. *J Magn Reson* 181:287–295
- Camaiti M, Casieri C, De Luca F, Fantazzini P, Terenzi C (2007) The use of portable single-sided relaxometry and laboratory imaging NMR devices in stone conservation. *Stud Conserv* 52:39–47
- Casieri C, Senni L, Romagnoli M, Santamaria U, De Luca F (2004) Determination of moisture fraction in wood by mobile NMR device. *J Magn Reson* 171:363–372
- Casieri C, De Luca F, Fantazzini P (2005) Pore-size evaluation by single-sided nuclear magnetic resonance measurements: compensation of water self-diffusion effect on transverse relaxation. *J Appl Phys* 97(043901):1–10
- Cignini R, Melzi R, Tedoldi F, Casieri C, De Luca F (2006) Large surface mapping by unilateral NMR scanner. *Magn Reson Imaging* 24:813–818
- Eidmann G, Savelsberg R, Blümmler P, Blümich B (1996) The NMR MOUSE, a mobile universal surface explorer. *J Magn Reson* 122:104–109
- Fechete R, Demco DE, Blumich B (2003) Order parameters of the orientation distribution of collagen fibers in Achilles tendon by H-1 NMR of multipolar spin states. *NMR Biomed* 16:479–483
- Ishimara Y, Arai K, Mizutani K, Oshima K, Lida I (2001) Physical and mechanical properties of wood after moisture conditioning. *J Wood Sci* 47:185–191
- Jakiela S, Bratasz L, Kozłowski R (2008) Numerical modelling of moisture movement and related stress field in lime wood subjected to changing climate conditions. *Wood Sci Technol* 42:21–37
- Kashyap R (1999) *Fiber Bragg Gratings*. Academic Press, New York
- Keckes J, Burgert I, Frühmann K, Müller M, Kölln K, Hamilton M, Burghammer M, Roth SV, Stanzl-Tschegg S, Fratzl P (2003) Cell-wall recovery after irreversible deformation of wood. *Nat Mater* 2:810–813
- Meiboom S, Gill D (1958) Modified spin-echo method for measuring nuclear relaxation times. *Rev Sci Instrum* 29:688–691
- Rao YJ (1999) Recent progress in applications of in-fiber Bragg grating sensors. *Opt Laser Eng* 31:297–324
- Reeb JE (1995) *Wood and moisture relationships*. Oregon State University Bulletin EM8600
- Senni L, Casieri C, Bovino A, Gaetani MC, De Luca F (2008) A portable NMR sensor for moisture monitoring of wooden works of art, particularly of painting on wood. *Wood Sci Technol* 43(1–2): 167–180
- Skaar C (1988) *Wood–water relations*. Springer, Berlin
- Viola I, Bubicci S, Casieri C, De Luca F (2004) The Codex Major of the Collectio Altaempsiana: a non-invasive NMR study of paper. *J Cult Herit* 5:257–261
- Wood Handbook: US Department of Agriculture (1987) *Wood as an engineering material*. Agriculture Handbook 72, Washington, DC